Title
STRESS CORROSION CRACKING OF ZIRCALOY BY CADMIUM, IODINE, AND METAL IODIDES

Authors
Sham, S.H.
Olander, D.R.

Publication Date
1982

LBL-13855
Preprint

Lawrence Berkeley Laboratory
UNIVERSITY OF CALIFORNIA

Materials & Molecular Research Division

Submitted to the Journal of Nuclear Materials

STRESS CORROSION CRACKING OF ZIRCALOY
BY CADMIUM, IODINE, AND METAL IODIDES

S.H. Shann and D. R. Olander

January 1982

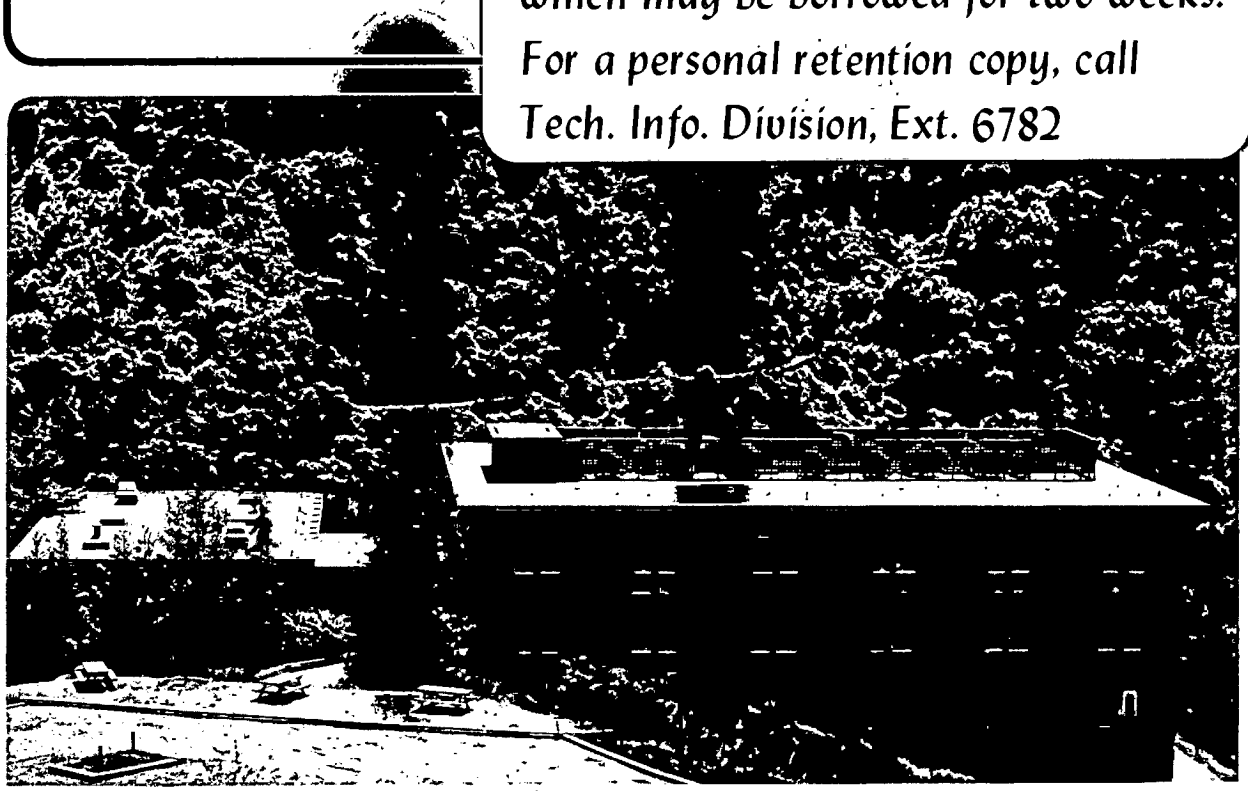

Prepared for the U.S. Department of Energy under Contract W-7405-ENG-48

DISCLAIMER

LBL-13855

STRESS CORROSION CRACKING OF ZIRCALOY BY CADMIUM, IODINE, AND METAL IODIDES

by S. H. Shann and D. R. Olander

Materials and Molecular Research
Division of Lawrence Berkeley
Laboratory and the
Department of Nuclear Engineering
University of California
Berkeley, California 94720

This work was supported by the Director, Office of Energy Research, Office of Basic Energy Sciences, Materials Sciences Division of the U.S. Department of Energy under contract # W-7405-ENG-48.

ABSTRACT

In order to examine the cause of the reactor fuel pin pellet-cladding interaction phenomenon (PCI), stress corrosion cracking (SCC) experiments of Zircaloy under iodine, iron iodide, aluminum iodide, cesium iodide, and cadmium were undertaken. Rupture lifetimes were measured as a function of stress, temperature, and the equivalent pressure of the corrosive agents. Tests with CsI and simultaneous irradiation were also performed to check whether radiation decomposition can induce Zircaloy SCC. Iodine, iron iodide, and aluminum iodide substantially reduced the failure times in comparison to those of control specimens at the same stress and temperature. A critical stress of $\sim$ 379 MPa for iodine and iron iodide separates burst type failure from low-stress short slit failures. Both types showed brittle cleavage fracture surfaces. The presence of cesium iodide did not have any influence on the failure time of Zircaloy. The failure was burst-type, and the fractography was ductile. Simultaneous radiation tests with cesium iodide did not cause reduction in failure time either. All specimens failed under cadmium vapor by a burst mode, but the fractography showed cleavage brittle characteristics and the failure times were much smaller than those of control specimens. The results indicate that neither elemental iodine nor its compounds are responsible for PCI failures. The most likely element for this role is cadmium.

I. INTRODUCTION

Since the earliest work by Rosenbaum, Davies and Pon(1), laboratory and in-reactor experiments designed to elucidate the mechanism of pellet-cladding interaction (PCI) fuel rod failures have concentrated almost exclusively on iodine. The assumption that this is the responsible chemical agent is contained in models of PCI which have been constructed for incorporation into fuel performance codes(2). The evidence implicating iodine is circumstantial, being based primarily upon the volatility and significant fission yield of this element and on the microstructural similarity of the failed Zircaloy specimens exposed to iodine in laboratory stress corrosion cracking (SCC) tests to cladding failures by PCI(2-6). The fission yield of cesium is many times larger than that of iodine and because of the great stability of the compound CsI, essentially all of the iodine inside an intact fuel rod is contained in this form. However, laboratory tests have demonstrated that CsI is <u>not</u> an SCC agent for Zircaloy. In order to prove that iodine is the element responsible for Zircaloy SCC inside a fuel pin one of the following conditions needs to be met.

First, although CsI is the dominant iodine-bearing species in irradiated fuel, a very small partial pressure of elemental iodine is predicted thermodynamically. Cubiocciotti, Jones and Syrett determined that CsI reaction with the fuel produces an iodine pressure of the order of 10^{-19} atm(7). Götzmann calculates an iodine pressure of $\sim 10^{-15}$ atm at 600 K for the reaction of cesium iodide with fission product molybdenum in stoichiometric urania(8). If iodine is the cause of fuel rod PCI failures, it must be capable of acting as an SCC agent to Zircaloy at extremely low pressure.

Second, on the basis of the observation of iodine release from gamma-irradiated cesium iodide crystals(9), radiolysis of cesium iodide has been proposed as a mechanism of liberating sufficient elemental iodine to produce stress corrosion cracking of the cladding of light water reactor fuel elements(7).

Both of these possibilities were examined in the present study. The role of iodine in promoting Zircaloy SCC has been reassessed using an experimental technique which permits direct control of the iodine partial pressure to which the Zircaloy is exposed, instead of the quantity of iodine per unit surface area used in previous work. The effects of temperature, applied stress and iodine partial pressure on the time-to-failure of biaxially-stressed Zircaloy tubes was determined.

Similar experiments were performed using the metal iodides FeI_2 and AlI_3 because Zircaloy cracking is frequently observed to be initiated near iron or aluminum impurity particles on the surface(10).

By coupling the stress corrosion cracking apparatus to an accelerator ion beam, the effect of irradiation on the SCC potential of cesium iodide was studied.

Finally, the ability of cadmium vapor to promote low-ductility failure of stressed Zircaloy was investigated and the relevance of the results to interpretation of PCI failures in reactor fuel pins is discussed.

II. EXPERIMENTAL

The apparatus shown in Fig. 1 consists of a closed resistively-heated Zircaloy tube specimen pressurized internally with argon to produce the desired hoop stress. This pressurized-tube test procedure produces a stress biaxiality ratio (hoop-to-axial) of two. The specimen

internal pressure is measured by a transducer and its temperature by a spring-loaded thermocouple contacting the outside surface near the middle of the tube. The specimen is housed in an evacuated chamber (10^{-6} Torr base pressure) and contains a loose-fitting glass rod to reduce the gas load on the vacuum pumps when failure occurs.

In all previous experimental studies of iodine SCC of Zircaloy a known quantity of iodine was added to the inside of the sealed tube. This procedure precluded control and even knowledge of the iodine pressure contacting the metal and led to the practice of describing iodine availability in the thermodynamically meaningless units of mg/cm^2. In the present experiment, iodine and other SCC agents were delivered to the outside surface of the tube specimen in the form of a molecular beam with a well-defined equivalent pressure. The molecular beam impinged on a spot $\sim$ 5 mm in diameter on the tube and failure always occured inside this spot. Iodine was delivered to the doser tube in Fig. 1 from a reservoir at controlled temperature. The equivalent iodine pressure was calculated from the flow rate through the doser tube and gas kinetic theory by the method described in Ref. 11. When the metal iodides (FeI_2, AlI_3 or CsI) or cadmium were tested, the doser in Fig. 1 was replaced by a Knudsen cell, which is a tube containing the solid with a small ($\sim$ 1 mm diameter) hole facing the Zircaloy tube surface. When heated to a temperature which produces the appropriate vapor pressure, a molecular beam of the desired species emerges from the hole and bombards the Zircaloy surface. The equivalent pressure of the molecular beam so formed is calculated from kinetic theory (11).

The tests with molecular iodine and aluminum iodide as SCC agents utilized stress-relieved Zircaloy-2 tubes from a lot supplied by SRI International which was similar to the tubing used in their study (12). However, most testing

was done on tubing obtained directly from Sandvik Special Metals Corp. The SRI specimens were 11.5 mm I.D. and the Sandvik material was 10.5 mm I.D. Both tubing specimens were mechanically thinned from the outside to give a wall thickness of 0.25 mm and were used without further treatment other than an alcohol wash. Several SRI specimens were mechanically preflawed by machining longitudinal notches 25 μm deep and 25 mm long on the outside surface. The experiments utilizing iron iodide, cesium iodide and cadmium were conducted with Sandvik stress-relieved Zircaloy-4 tubing. The I.D. of the tubes was 8.2 mm and the wall thickness was 0.64 mm. The material was used in the as-received condition.

Surfaces of some specimens after the tests were examined by Auger electron spectroscopy (AES) or energy dispersive analysis by X-rays (EDAX) for their elemental composition. Since the surface analysis equipment was not part of the SCC test apparatus, the specimens had to be removed from the latter and transported to the former, thereby becoming exposed to air. Zirconium and iron iodides on the Zircaloy surface react readily with air or water vapor and release iodine, so none of this element was observed on surfaces exposed to the atmosphere. Aluminum iodide and cesium iodide do not react in this manner, and iodine could be detected after the tests.

For testing the effect of irradiation on the SCC process with CsI, the flange shown on the left hand side of Fig. 1 was connected to a Van de Graaff accelerator which generated a 10 μa, 175 keV proton beam. The H^+ ion beam and the CsI molecular beam struck the same spot on the heated, stressed Zircaloy surface.

III RESULTS

In all experiments, the time-to-rupture was measured for various

combinations of stress, temperature, and pressure of the SCC agent. In addition, the rupture was characterized macroscopically as "burst" (large strain at failure) or "slit" (low-ductility failure in the form of a longitudinal slit 1-2 mm long). The "pinhole" type of breach reported by Jones et al.(13) and Syrett et al.(14) was not observed. Figure 2 shows a typical iodine SCC failure. The roughened zone around the slit is general corrosion which occurs within the confines of the iodine molecular beam spot. The fracture surface was characterized by scanning electron microscopy as "ductile-dimple" or "cleavage". In the latter case the surface features were characteristic of transgranular rather than intergranular failure. In both the macro- and micro-characterizations, the second features (slit on a macroscopic scale and cleavage on a microscopic level) are characteristic of stress corrosion cracking failure of the metal. A transition to ductile failure occurs when the SCC crack grows to a length at which the net section stress reaches approximately the ultimate tensile stress.

A. Iodine

Figure 3 shows the variation of the time-to-failure of the Sandvik specimens with nominal hoop stress at 573 K and constant I_2 equivalent pressure. At high stress, the failure time varies as σ^{-8} but appears to flatten out at a stress of $\sim$ 300 MPa, which is consistent with the threshold stress determined by Jones et al.(13,15) for similar tubing. However, the threshold stress may be dependent upon iodine availability; a specimen subjected to a lower iodine pressure (4×10^{-3} Torr instead of the 1.4×10^{-2} Torr for the test of Fig. 2) did not fail after 80 hours at 318 MPa.

All specimens exposed to iodine at stresses less than $\sim$ 370 MPa

(open circles in Fig. 2) exhibited slit failures and cleavage fracture surfaces. The control specimens (closed circles in Fig. 2) failed in a burst mode and the fracture surfaces showed ductile-dimple features. Two tests with iodine at 379 MPa (stars in Fig. 2) failed in the burst mode macroscopically but microscopically showed cleavage fracture surfaces. The rupture times for these two tubes fell between the iodine SCC curve and the line representing the control specimens. This behavior is consistent with the loss of effectiveness of iodine as an SCC agent at high hoop stresses observed by Jones et al.(13).

The temperature dependence of the failure time at fixed nominal stress and iodine equivalent pressure shown in Fig. 4 is described by an activation energy of 7 ± 1 kcal/mole. This value is considerably lower than that deduced from the SCC experiments in which a fixed quantity of iodine is sealed inside the tube with the pressurizing gas. This type of test gives activation energies of 30 kcal/mole(13,16).

The dependence of the failure time on equivalent iodine pressure for several combinations of hoop stress and temperature is shown in Fig. 5. The stress listed for the preflawed SRI specimens is the nominal rather than the net section stress. According to Jones et al.(15) the former as adequate a characterization of the true stress driving the SCC process as is the latter. The net section stress for the preflawed specimens in Fig. 5 is nearly equal to the nominal stress for the unflawed specimens. If the net section stress best represented the true stress, the failure times for both sets of data representing the SRI tubes should have been the same. The results shown on the plot clearly do not support this expectation; rather they are consistent with an interpretation of nominal hoop stress, not net section stress or stress intensity factor,

as the appropriate load variable for iodine SCC. This inference is substantiated by transferring the data from Fig. 5 for both SRI specimens at an iodine pressure of 1.4×10^{-3} Torr to the plot of Fig. 3 in which stress is the independent variable. Making the modest temperature correction to the failure times using the activation energy of 7 kcal/mole, agreement with the Sandvik specimen data on Fig. 3 is found to be good provided that the nominal stress is used for the preflawed specimen data.

The rupture times for the control specimens (no iodine) are indicated as horizontal lines in Fig. 5. The data show that the features of iodine SCC (i.e., reduction of rupture time, low-ductility failure with a cleavage fracture surface) appear at an equivalent iodine pressure just a bit greater than 10^{-3} Torr (2×10^{-6} atm). It is not possible to compare this iodine threshold of the SCC process with the minimum iodine "availability" quoted in previous studies (Ref. 4, for example). In these cases, the iodine concentration was reported either on an areal basis or as the hypothetical iodine pressure which would have prevailed if no iodine reaction with the specimen had occurred. Least-squares fitting of the data in Fig. 5 for all three specimens tested yields a slope of -1 ± 0.1 for the lines on the log-log plots of failure time versus iodine equivalent pressure.

The iodine SCC data collected in this investigation can be represented by the equation:

$$t_F \propto \sigma^{-8} \, p_{eq}^{-1} \, e^{3500/T}$$

where σ is the nominal hoop stress, p_{eq} is the equivalent pressure of iodine and T is the absolute temperature. This formula is valid for the stress range $300 < \sigma < 380$ MPa, beyond which iodine SCC does not occur.

B. Aluminum Iodide

Experiments utilizing AlI_3 as the SCC agent were conducted with Sandvik tubing at a fixed nominal hoop stress (365 MPa) at one temperature (573 K). Figure 6 shows the effect of AlI_3 pressure on the failure time. The minimum pressure which causes SCC failure under these conditions is $\sim 10^{-3}$ Torr, close to that observed for iodine. At higher AlI_3 pressures, the rupture time decreases according to the function:

$$t_F \propto p_{eq}^{-2/3}$$

Both burst and slit failure modes were observed, but all fracture surfaces were of the brittle cleavage type.

After the experiments, the specimens were split along the crack, mounted and examined by EDAX for the distribution of aluminum and iodine on the fracture surface. The results are shown in Fig. 7 for various locations on the cracks of four of the specimens which failed by SCC. Although the scatter of these data is considerable, the trend of decreasing concentration with increasing distance from the surface exposed to the AlI_3 beam is clearly established. The iodine concentration gradient is less steep than that of aluminum. These results suggest that a transport process, most likely surface diffusion, controls the rate of supply of the corrosive agents to the advancing tip. The more pronounced decrease in the aluminum signals than those from iodine with distance along the crack surface means that the Al:I ratio decreases along the crack. This suggests that the two elements migrated from the surface to the crack tip at least in part as independent species and do not maintain the constant 1:3 atom ratio of the gas phase aluminum iodide which supplies the exterior surface.

The open circles in Fig. 6 represent specimens which did not fail in 43 hours when subjected to AlI_3 pressures less than 10^{-3} Torr. However, all three specimens exhibited longitudinal nonpenetrating cracks on the surfaces exposed to the beam. The density of these embryo cracks (see Fig. 8) suggests that crack initiation was not limiting the SCC process and that slow crack propagation was at least in part responsible for determining the absence of failure in the 43 h testing period.

C. Iron Iodide

In this test series the SCC agent was gaseous FeI_2 which impinged as a molecular beam on the outer surface of stress-relieved Zircaloy-4 tube specimens. Figure 9 shows the stress dependence of the failure time at 623 K in the absence of the SCC agent and in the presence of an FeI_2 equivalent pressure of 9×10^{-3} Torr. All specimens exposed to FeI_2 showed substantial reduction of the failure time compared to the control specimens and the fracture surfaces of the former were all of the brittle-cleavage type. However, tubes with hoop stresses greater than 379 MPa failed in the burst mode macroscopically whereas those subjected to lower stresses exhibited slit fractures with very little gross strain. This feature of the FeI_2 data is identical to that observed using iodine as the SCC initiator. However, failure times in iron iodide were much more sensitive to stress than those with iodine.

The temperature dependence of the failure time shown in Fig. 10 corresponds to an activation energy of 131 kcal/mole, which is very much larger than the 7 kcal/mole observed with iodine.

The FeI_2 pressure effect shown in Fig. 11 suggests a minimum pressure

of $\sim 10^{-3}$ Torr for the onset of SCC and a decrease with an exponent -0.9 ± 0.1 at higher pressures. This result is the same as that found for I_2 but is different from AlI_3.

The FeI_2 results for Zircaloy-4 can be summarized by the equation:

$$t_F \propto \sigma^{-20}\ p_{eq}^{0.9}\ e^{66000/T}$$

In order to help clarify the relative significance of crack initiation and crack propagation, a specimen was subjected to a stress of 376 MPa at 623 K and $p_{eq} = 9 \times 10^{-3}$ torr FeI_2. The tube was removed after 3 hr of testing, which is $\sim$ 20% of its failure time under these conditions (Fig. 10). The outer tube surface at the beam spot was examined by scanning Auger electron microscopy in a system which was also capable of removing surface material by ion sputtering.

The specimen surface prior to ion milling showed only iron and oxygen by elemental analysis. Cracks were visible on this corrosion coat. After removal of $\sim$ 0.5 μm of the surface by sputtering, low-spatial-resolution AES showed only zirconium. Figure 12 shows that a significant density of nonpenetrating cracks were still evident. These cracks therefore penetrated partially into the Zircaloy. Examination of individual cracks with high-spatial-resolution AES showed all to be associated with high signals of iron and tin, in agreement with the findings of Cubiocciotti et al.(10). A high magnification view of the large crack in the center of the upper photo is shown in the lower part of Figure 12.

One of the cracks in Fig. 12 would undoubtedly have become enlarged and ultimately penetrated the tube wall had the SCC test been continued to the normal failure time under these conditions. This propagation step would have required at least 80% of the tube lifetime, which indicates that

initiation of cracks does not determine the time to failure, as has been suggested by Roberts et al.(15).

D. Cesium Iodide

Zircaloy-4 specimens were tested at 623 K with a molecular beam of CsI of 1.5×10^{-3} Torr equivalent pressure impinging on the surface. Posttest EDAX analysis of the fracture surface and the tube O.D. within the beam spot revealed both cesium and iodine in approximately a 1:1 atomic ratio. However, for hoop stresses between 370 and 390 MPa, the failure times fell on the curve for control specimens at the same temperature but without CsI. Except for the presence of white deposits of CsI visible by scanning electron microscopy, the fracture surfaces of the specimens which failed in CsI were indistinguishable from those of the control tubes. Cesium iodide by itself has no effect on creep rupture of Zircaloy. It does not induce stress corrosion cracking.

In order to determine whether there is a synergistic effect of simultaneous irradiation and cesium iodide exposure during testing, a 10 μa, 175 keV H^+ beam from an accelerator bombarded the same spot on the tube surface as was illuminated by the CsI molecular beam. However, before undertaking testing with both molecular and ion beams, the effect of irradiation alone was investigated. The accelerator beam bombarded a tube held at 623 K and 386 MPa stress for a series of 8 hour periods interspersed with 16 hour off times until failure occurred. In this interrupted mode of testing, the failure time of the irradiated specimen was 22.7 hr, compared to 24.3 hr for the control specimens continuously heated and stressed without irradiation. The irradiated specimen failed in a burst mode and showed a ductile dimple fracture surface. This test showed that the step-function mode of testing is equivalent to the

continuous mode and that proton irradiation of the metal surface has no effect on the rupture properties of Zircaloy.

Variation of the equivalent pressure in the irradiation tests is essential to discovering if radiation can convert normally innocuous CsI to an SCC agent for Zircaloy. If the equivalent pressure is too low, CsI molecules striking the surface will immediately evaporate, leaving little or none of this substance on the surface for the proton beam to interact with. At the other extreme, too large a molecular beam intensity will produce a thick scale of CsI and the proton beam will not penetrate to the scale-Zircaloy interface where radiation decomposition must take place if it is to promote SCC. The range of 175 keV protons in solid CsI was calculated from the Northliffe and Schilling tables(16) to be 3 μm.

The thickness of the scale during each test is calculated by estimating the rate of scale growth and multiplying by the test duration. The rate at which a CsI film grows on the metal is the net CsI flux to the surface divided by the density of solid CsI. The CsI flux consists of three components. The molecular beam supplies cesium iodide at a rate given by:

$$J_{beam} = \frac{p_{eq}}{(2\pi\ mkT)^{\frac{1}{2}}} \qquad (1)$$

where p_{eq} is the equivalent pressure of CsI, m is the mass of a molecule of CsI, and k is Boltzmann's constant. This equation assumes that the sticking probability of CsI on the metal surface is unity.

Again assuming unit condensation coefficient, the rate of vaporization of bulk CsI is:

$$J_{evap} = \frac{p_{vap}}{(2\pi\ mkT)^{\frac{1}{2}}}$$

where p_{vap} is the vapor pressure of solid CsI. This formula gives $J_{evap} = 4 \times 10^{14}$ molecules/cm^2-s at 623 K.

Cesium iodide can be sputtered by the proton beam. For 10 μa of 175 keV H^+, Smith's model(17) gives a sputtering rate of:

$$J_{sput} = 2.1 \times 10^{16} \text{ molecules/cm}^2\text{-s}.$$

The rate of growth of the CsI film thickness, δ, is:

$$\frac{d\delta}{dt} = \frac{J_{beam} - J_{evap} - J_{sput}}{\rho}$$

where ρ is the density of solid CsI. If the numerator of this equation is negative, no CsI exists on the surface (except perhaps for monolayer or submonolayer quantities bound to the Zircaloy more strongly than binding in bulk CsI).

Tube burst tests for CsI equivalent pressures from 10^{-5} to 10^{-3} Torr with simultaneous proton irradiation were conducted. None of the specimens tested failed in 22 hr, which is when all tests were terminated (the control specimen failed at 22.7 hrs). The presence of CsI films on the Zircaloy substrates was assessed experimentally by four methods.

First, the specimens were mounted in resin, cut and polished at the beam spot and the film thickness measured in an optical microscope. Second, the specimens were observed during the test. During ion bombardment of insulating targets (such as CsI), a blue light appears because of discharging of the potential built up by collection of the charged particles on the solid. On a metal target, no blue light is visible. Third, the beam spot was examined visually after each test. A CsI film is often seen as a white deposit. Finally, the specimens were

examined by SEM and EDAX.

Table 1 shows the results of these tests. Specimens subjected to CsI equivalent pressures of 10^{-4} Torr or less showed no evidence of a CsI film by any of the tests described above. The tests conducted at an equivalent pressure of 10^{-3} Torr revealed a 30 μm thick film after the experiment, which compares well with the calculated thickness of 34 μm. However, this film is ∿ 10 times thicker than the range of bombarding protons in CsI, so that none of the beam reached the CsI/Zircaloy interface. The test with a CsI beam equivalent to a pressure of 4×10^{-4} Torr gave positive indications of CsI in three of the four tests, but the film could not be found by optical microscopy. The calculated film thickness for this pressure was 3 μm. This thin scale may have been lost during the mounting and polishing operations.

If an irradiation enhancement of CsI stress corrosion cracking is present, it should have been observed in the tests at 4×10^{-4} or 10^{-4} Torr equivalent pressures, for in this range the film thickness should have been smaller than the range of protons in solid CsI. The dose rate to the tube surface to a depth equal to the ion range was calculated to be 2×10^{8} rad/s for the accelerator proton beam used in the tests. For comparison, the dose rate due to recoil fission fragments on the inner surface of the cladding of a fuel element in typical LWR operating conditions was computed to be 2×10^{6} rad/s (11). Thus despite an energy deposition rate ∿ 100 times larger than that delivered to cladding by fission fragments and a 100 fold range of CsI availability, no irradiation initiation of SCC of Zircaloy by cesium iodine was observed in our experiments.

E. Cadmium

The effect of cadmium vapor on the failure time and fracture mode of Zircaloy-4 was investigated at equivalent pressures between 2×10^{-3} Torr and 1.6×10^{-2} Torr. Although tube failures with cadmium showed many of the features found with iodine and the metal iodides, there were two distinctive differences. First, although all specimens exposed to cadmium which resulted in reduced failure times showed cleavage fracture surfaces by SEM examination, the macroscopic character of the rupture at all stresses was of the burst type. In the cases of iodine and iron iodide, burst failure with SCC microscopic fracture features occurred only at high stresses.

Second, the measured failure times showed considerably more scatter than those observed with the other SCC agents even though all specimens were taken from the same lot of Zircaloy. This variability was somewhat reduced by using specimens cut from the same tube (each of which was 1 m long). The poorer reproducibility of the data is seen in Fig. 13, in which data from three tubes are shown. These data show that the failure time-stress line is much flatter for cadmium than it is for iodine or iron iodide. This feature of the cadmium-Zircaloy interaction means that small errors in the hoop stress (due to minor variations in wall thickness at the beam spot, for example) are manifest as large changes in failure time.

Another difference between cadmium and the other species tested is the location of the fracture surface in the beam spot. In iodine and metal iodide SCC, failure invariably occurred at the center of the spot where beam impingement rate was the highest, whereas with cadmium, failures occurred randomly inside the entire zone defined by the size of the beam spot. This behavior suggests a greater sensitivity to surface chemical or

physical inhomogeneities for cadmium SCC than for fracture caused by iodine or the metal iodides. Such an effect could also result in exaggerated scatter of the failure time between different tubes from the same lot.

Figure 13 demonstrates the deleterious effect of low pressure cadmium vapor on the burst properties of Zircaloy, with reductions in failure time typically a factor of ten. The cleavage fracture surfaces are decorated with white deposits which were shown by EDAX to correspond to the known intermetallic compounds ZrCd and Zr_2Cd. The cadmium concentration on the remainder of the fracture surface was less than 5 atom percent.

The dependence of failure time on equivalent pressure at 623 K and 380 MPa stress is shown in Fig. 14 for specimens taken from two tubes. For both sets of data, the relationship

$$t_F \propto (p_{eq})^{-1\pm0.2}$$

was found. The separation of the two lines is attributed to the tube-to-tube variability discussed above.

The temperature dependence of the failure time (Fig. 15) exhibits a feature not found in the tests with iodine and the metal iodides. The $\ln t_F$ - 1/T type of temperature dependence of the rupture time seen in Figs. 4 and 10 occurs only over a narrow temperature range with cadmium. Within this window, the activation energy is 54 ±2 kcal/mole. The width of the window becomes narrower as the equivalent pressure decreases and disappears entirely for $p_{eq} = 2 \times 10^{-3}$ Torr. This minimum pressure for SCC of Zircaloy is close to that found for iodine and the metal iodides. Even at higher equivalent pressures, the failure time returns to that

observed in control specimens at high temperature, presumably because cadmium striking the Zircaloy surface immediately vaporizes. The SCC features of the rupture also disappear at low temperatures, probably because the Cd-Zr interaction which is a prerequisite for SCC is kinetically limited and cadmium simply collects harmlessly on the Zircaloy surface as does cesium iodide. A temperature window for cadmium liquid metal embrittlement has also been observed(18). It is of interest to note that iodine SCC of Zircaloy also has an upper temperature limit; Hofmann(19) has shown that iodine has no effect on the burst properties of Zircaloy for temperatures greater than $\sim$ 1100K. The temperature window for cadmium may simply be narrower than those of the other SCC agents tested.

IV DISCUSSION

A. Chemical Aspects of Zircaloy SCC

Stress corrosion cracking of Zircaloy by gaseous iodides is a complex blend of heterogeneous chemistry and fracture mechanics. Because practically nothing is known about the mechanisms of the reactions of iodine and the metal iodides with zirconium, the chemical aspects of the process can only be vaguely outlined.

The reason that elemental iodine, iron iodide and aluminum iodide are active stress corrosion cracking agents for Zircaloy whereas cesium iodide is not is a direct reflection of the stability of the iodides with respect to zirconium iodide. The most likely iodide produced on a zirconium surface attacked by low pressure of iodine-bearing gases is the monoiodide ZrI (Cubicciotti(7) reports the monoiodide to have an I/Zr ratio of 1.1, but the perfectly stoichiometric designation will be used in the following discussion). The equilibrium pressure of elemental

iodine over the two-phase Zr/ZrI solid mixture is $\sim 10^{-15}$ atm at 600 K(7,8), so that any iodine pressure greater than this will convert Zr to ZrI. A rough measure of the relative stability of metal iodides with respect to ZrI is afforded by the standard free energy change of the reaction:

$$\frac{1}{n} MI_n(g) + Zr(s) = ZrI(s) + \frac{1}{n} M(s)$$

This calculation requires combining the equilibrium iodine pressure over the two-phase solid mixture Zr/ZrI with the free energies of formation of the iodides MI_n(20). The free energy changes for M = Fe and M = Al at 600 K are found to be -33 and -11 kcal/mole, respectively, whereas that for M = Cs is +29 kcal/mole. Thermodynamically at least, zirconium metal can decompose AlI_3 and FeI_2 and thereby release iodine for formation of zirconium iodide, which is presumably a prerequisite for stress corrosion cracking. Cesium iodide, on the other hand, will not react with zirconium.

The above calculation is about all of the assistance that thermochemistry can offer in elucidating the SCC process. Further understanding requires consideration of the rates of the steps involved. Some evidence bearing on the pertinent chemical kinetics is contained in the activation energies and equivalent pressure dependences determined experimentally. For iodine, the failure time varies inversely as the equivalent iodine pressure, which is indicative of a linear mechanism. In addition, the activation energy for iodine SCC is $\sim$ 7 kcal/mole. The linear pressure dependence and the low activation energy suggest that the rate-controlling step is associated with a gaseous diffusion or perhaps surface diffusion process. Stress corrosion cracking by FeI_2 is also linear but its very large activation energy (131 kcal/mole) can only be attributed to a rate-

controlling solid state diffusion or chemical reaction step. The activation energy for AlI_3 SCC was not measured, but the variation of the failure time with $p_{eq}^{2/3}$ rules out a rate-limiting diffusional step.

B. Minimum Iodine Pressure for Zircaloy SCC

Justification of the role of elemental iodine in pellet-cladding interaction (PCI) failures of LWR fuel elements is sometimes based on the presumption of an equilibrium chemical reaction involving the fuel or fission products which decomposes sufficient CsI to produce the requisite iodine pressure. The largest equilibrium pressure believed possible is $\sim 10^{-15}$ atm at 600 K(8). Using this pressure for p_{eq} in Eq(1) and estimating the projected area of an iodine atom to be 12 Å^2, three months would be required for a monolayer of iodine to form on the inner surface of the cladding of a fuel element. It is unlikely that an iodine pressure of this magnitude could be responsible for PCI. The results of the present work place the minimum iodine pressure for Zircaloy SCC at about 10^{-6} atm. Iodine pressures of this magnitude are not present inside irradiated fuel(21), nor, as shown in this study, can direct charged particle bombardment of surface-absorbed CsI liberate sufficient free iodine to produce an iodine potential equivalent to the minimum required pressure for SCC. If iodine is indeed responsible for PCI, the basic mechanism is still unknown, for none of the current explanations appear to be tenable.

C. Cadmium

Contrary to the controversy concerning the chemistry of iodine inside a fuel pin, the elemental state of cadmium is indisputable. The present study has shown that low pressures of this element can produce the micro-

scopic features and diminished failure times which are commonly offered in justification of iodine-induced PCI failures. Moreover, the temperature window in which the cadmium SCC process operates encompasses typical cladding temperatures. The major discrepancy between the specimens failed in laboratory tests with cadmium vapor and actual PCI failures is the type of gross tube breach. All cadmium SCC failures were found to be of the burst type, whereas PCI produces fine cracks in the cladding(22). However, there have been no laboratory tests with cadmium vapor on irradiated Zircaloy, which may behave differently from the unirradiated material used in this study. Support for this supposition is found in the study of Tomalin, Adamson and Gangloff(23), who determined that contact of irradiated Zircaloy specimens with solid cadmium in mandrel SCC tests produced PCI-type failures.

Cadmium is often dismissed as a possible cause of PCI failures because of its low fission yield ($\sim$ 0.1%). However, it is a straightforward matter to show that if all of the fission product cadmium in a 1 cm I.D. fuel pin with 90% smeared density was released to the void spaces, the cadmium pressure would attain the vapor pressure at 623 K (0.25 Torr) after a burnup of 0.15 MWd/tonne. Even if a substantial fraction of the cadmium is not released from the fuel, there clearly is enough of this element to exceed the minimum pressure for SCC found in this work (2×10^{-3} Torr), particularly for fuel burnups of tens of thousands of MWd/tonne.

V. CONCLUSIONS

Tube burst SCC tests of Zircaloy with gaseous I_2, FeI_2, and AlI_3 showed different activation energies and gas pressure and stress

dependences of the failure time. These differences reflect different mechanisms applicable to the three SCC agents; iron and aluminum do not merely act as inert carriers of iodine to the Zircaloy surface. The minimum pressure of any of these species required to produce SCC of Zircaloy is $\sim 10^{-6}$ atm. The time to failure in the tests was found to be determined more by crack propagation than by crack initiation.

Cesium iodide did not produce stress corrosion cracking of Zircaloy, even when subjected to intense ion radiation from an accelerator. Iodine SCC of fuel cladding by radiation decomposition of cesium iodide cannot be justified.

Cadmium SCC of Zircaloy reproduced many of the features of PCI failures of fuel pins and this fission product is a strong contender for the responsible element in low ductivility cladding failures.

ACKNOWLEDGEMENT

The helpful comments by Dr. Robin Jones of E.P.R.I. and of Dr. Barry Jones of the Central Electricity Generating Board are gratefully acknowledged. This work was supported by the Director, Office of Energy Research, Office of Basic Energy Sciences, Materials Sciences Division of the U.S. Department of Energy under contract #W-7405-ENG-48.

Table 1. Irradiation + CsI test results: Specimen conditions: 386 MPa and 623 K; Proton beam: 175 keV, 10 μa; failures: none in 22 hours

CsI equivalent pressure, torr	10^{-3}	4×10^{-4}	10^{-4}	5×10^{-5}	10^{-5}
CsI film thickness on posttest surface (μm)	30	0	-	-	-
Calculated CsI film thickness (μm)	34	3	0	0	0
Blue light during irradiation?	yes	yes	no	no	no
visual - white deposits?	yes	yes	no	no	no
SEM/EDAX	-	yes	-	no	no

REFERENCES

1. H. S. Rosenbaum, J. H. Davies and J. O. Pon, "Interaction of Iodine with Zircaloy-2", GEAP-5100-5 (1966).
2. A. K. Miller, K. D. Challenger and A. Tasooji, "SCCIG: A Phenomenlogical Model for Iodine Stress Corrosion Cracking of Zircaloy", EPRI NP-1798 Volume 1 (1981).
3. C. C. Busby, R. P. Tucker, and J. E. McCauley, J. Nucl. Mater., 55 (1975) 64.
4. M. Peehs, H. Stehle, and E. Steinberg, "Out-of-Pile Testing of Iodine Stress Corrosion Cracking in Zircaloy Tubing in Relation to the Pellet-Cladding Interaction Phenomenon", ASTM STP-681, (1979) 244.
5. B. Cox and J. C. Wood, "Iodine Induced Cracking of Zircaloy Fuel Cladding", Proc. Conf. of the Corrosion Division of the Electrochemical Soc., Corrosion Problems in Energy Conversion and Generation, C. S. Tedman, Ed. (1974) 275.
6. F. Garzarolli, R. von Jan and H. Stehle, At. Energy Rev. 17 (1979) 1.
7. D. Cubicciotti, R. L. Jones, and B. C. Syrett, "Chemical Aspects of Iodine-Induced Stress Corrosion Cracking of Zircaloy," ASTM Fifth Conference on "Zirconium in Industry," 1980.
8. O. Götzmann, "Evolution of Iodine Potentials in LWR Fuel Rods Relevant to PCI Failures", paper presented at the ANS/ENS Topical Meeting on Reactor Safety Aspects of Fuel Behavior, Sun Valley, Idaho, August 2 - 6 (1981).
9. D. Cubicciotti and J. H. Davis, Nucl. Sci. Eng., 60 (1976) 314.
10. D. Cubicciotti, S. M. Howard and R. L. Jones, J. Nucl. Mater., 78 (1978) 2.

11. S. H. Shann, "Radiation Enhancement of Stress Corrosion Cracking of Zircaloy", PhD thesis, LBL-13200 (1981).

12. D. Cubicciotti and R. L. Jones, "EPRI-NASA Cooperative Project on Stress Corrosion Cracking of Zircaloys", EPRI NP-717 (1978).

13. R. L. Jones, D. Cubicciotti and B. C. Syrett, J. Nucl. Mater., 91 (1980) 277.

14. B. C. Syrett, D. Cubicciotti and R. L. Jones, J. Nucl. Mater. 92 (1980) 89.

15. J. T. A. Roberts, R. L. Jones, D. Cubicciotti, A. K. Miller, H. F. Wachob, E. Smith and F. L. Yagee, "A Stress Corrosion Cracking Model for Pellet-Cladding Interaction Failures in Light-Water Reactor Fuel Rods", STP 681, Amer. Soc. for Testing and Mater., (1979) 285.

16. L. C. Northliffe and R. F. Schilling, Nuclear Data Tables, A7 (1970) 233.

17. D. L. Smith, J. Nucl. Mater., 75 (1978) 20.

18. C. F. Old, "Liquid Metal Embrittlement of Nuclear Materials," J. Nucl. Mater., 92 (1980) 2.

19. P. Hofmann, J. Nucl. Mater.,87 (1979) 49.

20. O. Kubaschewski and C. B. Alcock, Metallurgical Thermochemistry", 5th Ed. Pergamon Press (1979).

21. J. H. Davies, F. T. Frydenbo and M. B. Adamson, J. Nucl. Mater., 80 (1979) 366.

22. F. Garzarolli, R. von Jan and H. Stehle, Atomic Energy Review 17 (1979) 31.

23. D. S. Tomalin, R. B. Adamson and R. P. Gangloff, "Performance of Irradiated Copper and Zirconium Barrier-Modified Zircaloy Cladding Under Simulated Pellet-Cladding Interaction Conditions", STP 681, Amer. Soc. for Testing and Mater., (1979) 122.

Figure Captions

1. Apparatus for studying stress corrosion cracking of Zircaloy by gaseous chemicals. The system shown is for use with elemental iodine. For less volatile species, the doser is replaced by a Knudsen Cell.
2. Spot on the surface of a Zircaloy tube which had been exposed to a molecular beam of iodine of 0.014 Torr equivalent pressure for 9 hours. The tube was stressed to 369 MPa(hoop) and held at 573 K during the test. The low-ductility failure is visible as an axial slit $\sim$ 1 mm long.
3. Stress dependence of Sandvik Zircaloy-2 tube failure times with and without iodine at 573K. The ultimate tensile strength of the material is indicated by the arrow on the ordinate.
4. Temperature dependence of Sandvik Zircaloy-2 tube failure times for a nominal hoop stress of 314 MPa and an equivalent iodine pressure of 1.4×10^{-2} Torr.
5. Iodine equivalent pressure dependence of the failure time of Zircaloy-2 tubing. The horizontal lines labeled "no iodine" give the failure times of control specimens under the same temperature and loading conditions.
6. Effect of AlI_3 equivalent pressure on the failure time of Zircaloy-2 tubing. The line has a slope of -2/3.
7. EDAX signals moving from outside surface of the tube along the fracture surface of stress corrosion cracks. C_{Al} is the aluminum signal, C_I is that for iodine and C_{tot} is the total signal for all elements. For different positions on the following specimens

   $P_{eq} = 1.4 \times 10^{-3}$ Torr, $t_f = 36.7$ hrs: ▼ ■ ◆

   $P_{eq} = 2 \times 10^{-3}$ Torr, $t_f = 9.4$ hrs: O X Δ ∇

   $P_{eq} = 5 \times 10^{-3}$ Torr, $t_f = 4.8$ hrs: □ ◇ +

   $P_{eq} = 2 \times 10^{-2}$ Torr, $t_f = 2.9$ hrs: ▲

8. Small crack in the outer surface of an unfailed Zircaloy-2 tube which had been subjected to a nominal hoop stress of 365 MPa and 3.3×10^{-4} Torr pressure of AlI_3 at 573 K for 43 hours.
9. Stress dependence of the failure times of Zircaloy-4 tubes with and without exposure to FeI_2 at 623 K. The ultimate tensile strength of the material is indicated as the arrow on the ordinate.
10. Temperature dependence of the failure time of Zircaloy-4 tubes exposed to FeI_2.
11. Variation of the failure time of Zircaloy-4 tubes with equivalent pressure of FeI_2 at fixed stress and temperature. The arrow indicates the rupture time of the control specimen under the same conditions but without corrosive agent.
12. Scanning Auger microsopy of nonpenetrating cracks on the surface of a Zircaloy-4 tube which had been exposed to FeI_2 for 20% of its failure lifetime. The specimen was ion-sputtered on the beam spot until the Zircaloy signal from the low resolution picture (top) was that of the substrate Zircaloy. The high resolution image of a large crack (bottom) showed a strong iron signal by Auger analysis.
13. Rupture times of three Zircaloy-4 tubes from the same lot with and without cadmium exposure.
14. Effect of equivalent pressure of cadmium on the failure times of specimens cut from two Zircaloy-4 tubes.
15. Temperature effect on Zircaloy-4 failure times at four cadmium equivalent pressures. The lifetimes of control specimens follow the straight line in the plot. Reduction in tube lifetime occurs only over a range of temperatures which becomes narrower as the equivalent cadmium pressure is reduced, eventually disappearing at a pressure of 2×10^{-3} Torr.

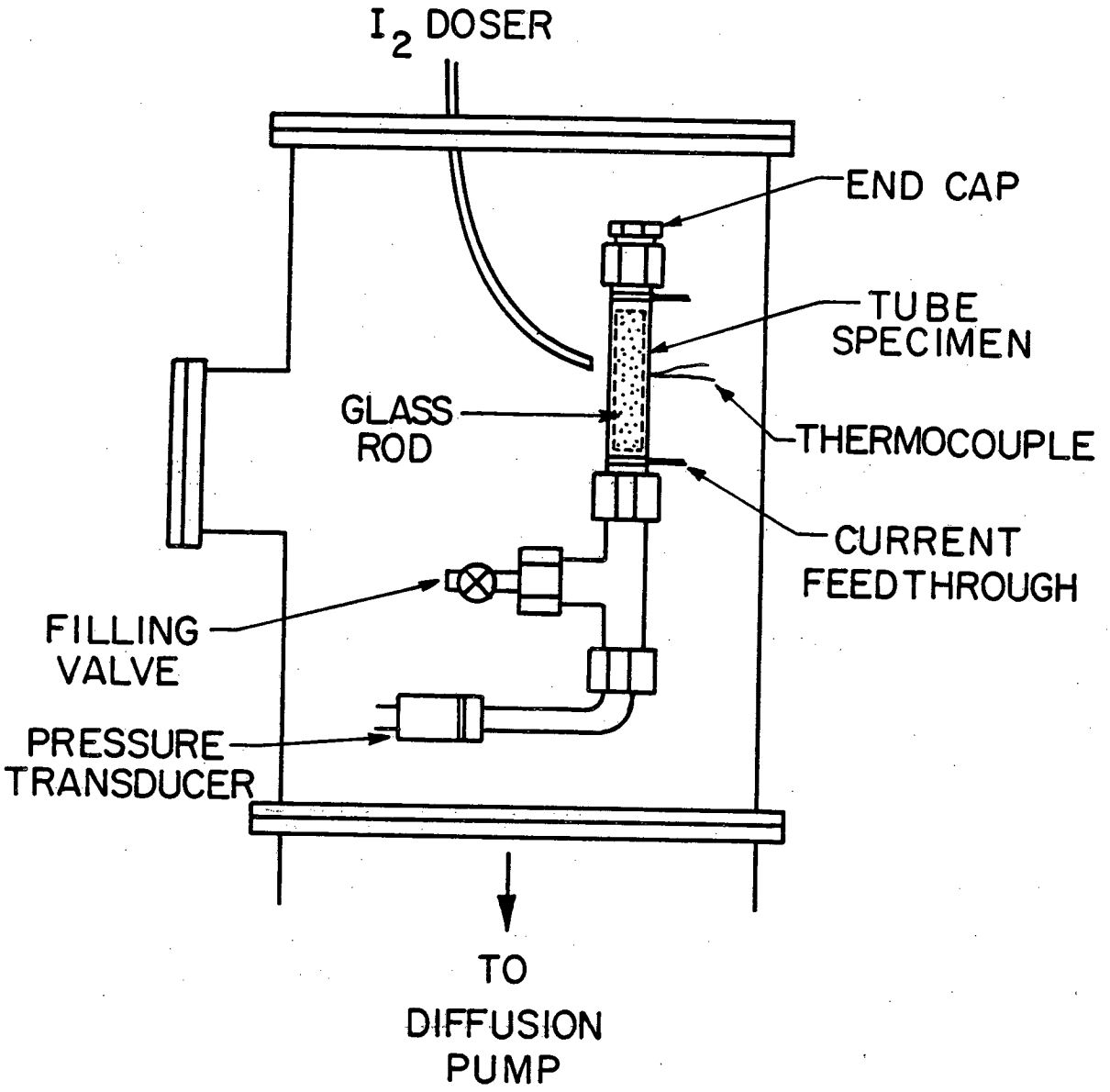

Figure 1. Iodine stress corrosion cracking apparatus.

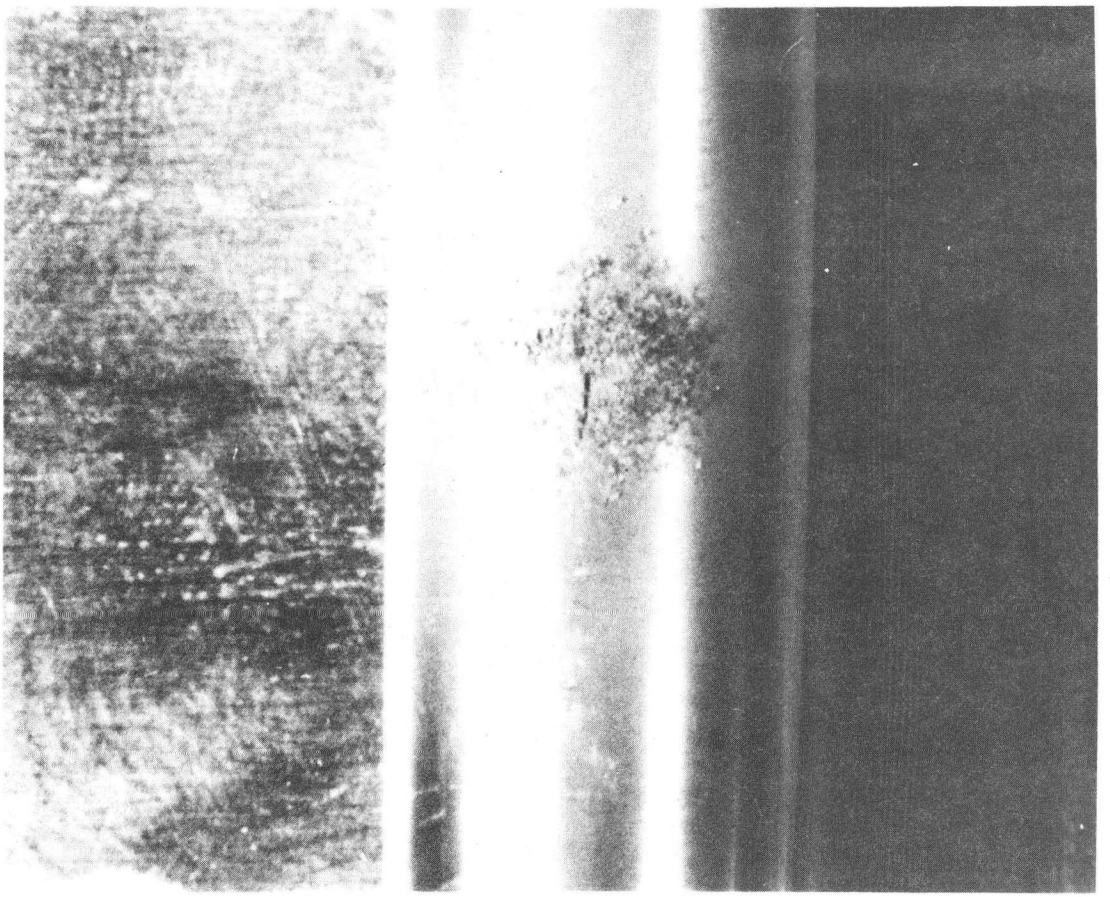

XBB 791-474

Fig. 2 Sandvik Zircaloy-2 specimen failed after 9 hours under 369 MPa stress and 0.014 Torr iodine pressure at 573 K

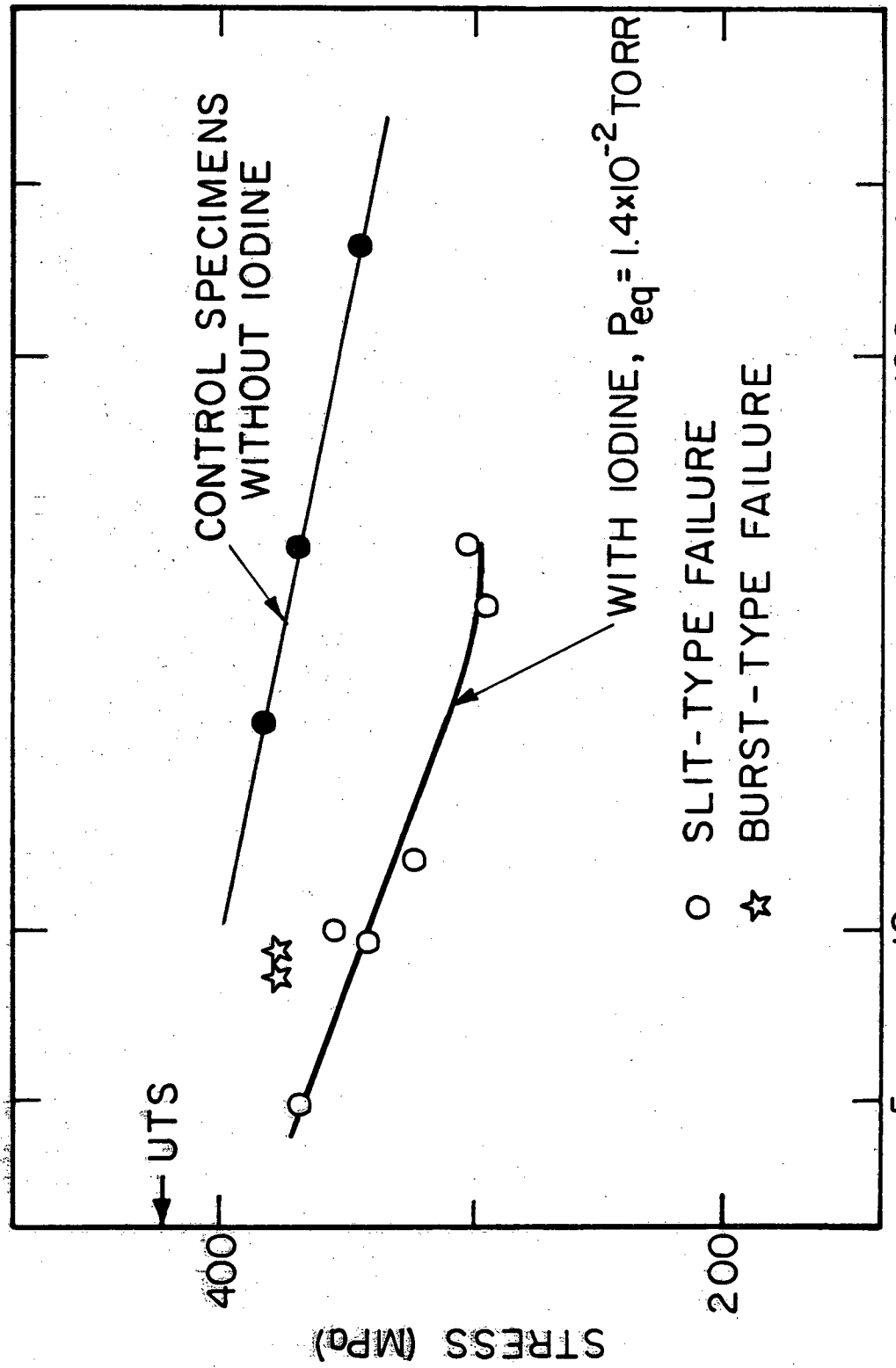

XBL812-5220B

Fig. 3

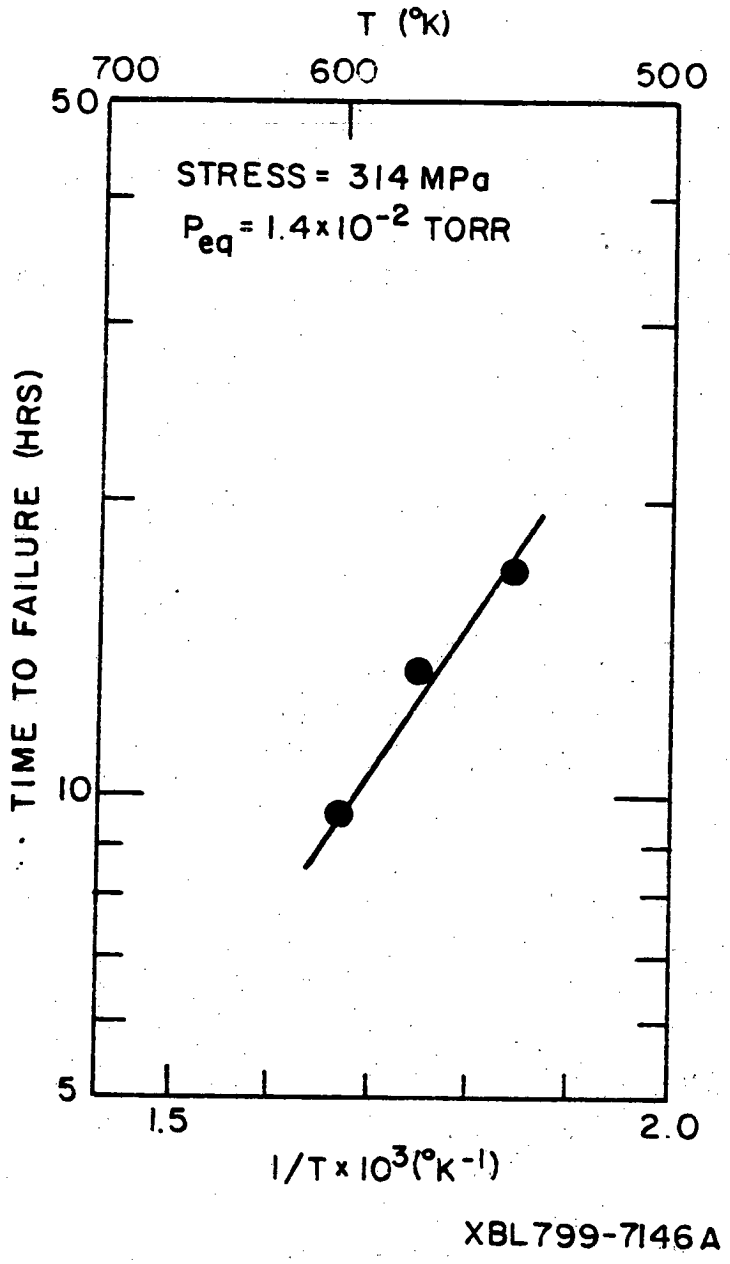
T (°K)
700
600
500
50
STRESS = 314 MPa
$P_{eq} = 1.4 \times 10^{-2}$ TORR
TIME TO FAILURE (HRS)
10
5
1.5
2.0
$1/T \times 10^3 (°K^{-1})$
XBL799-7146A

Figure 4

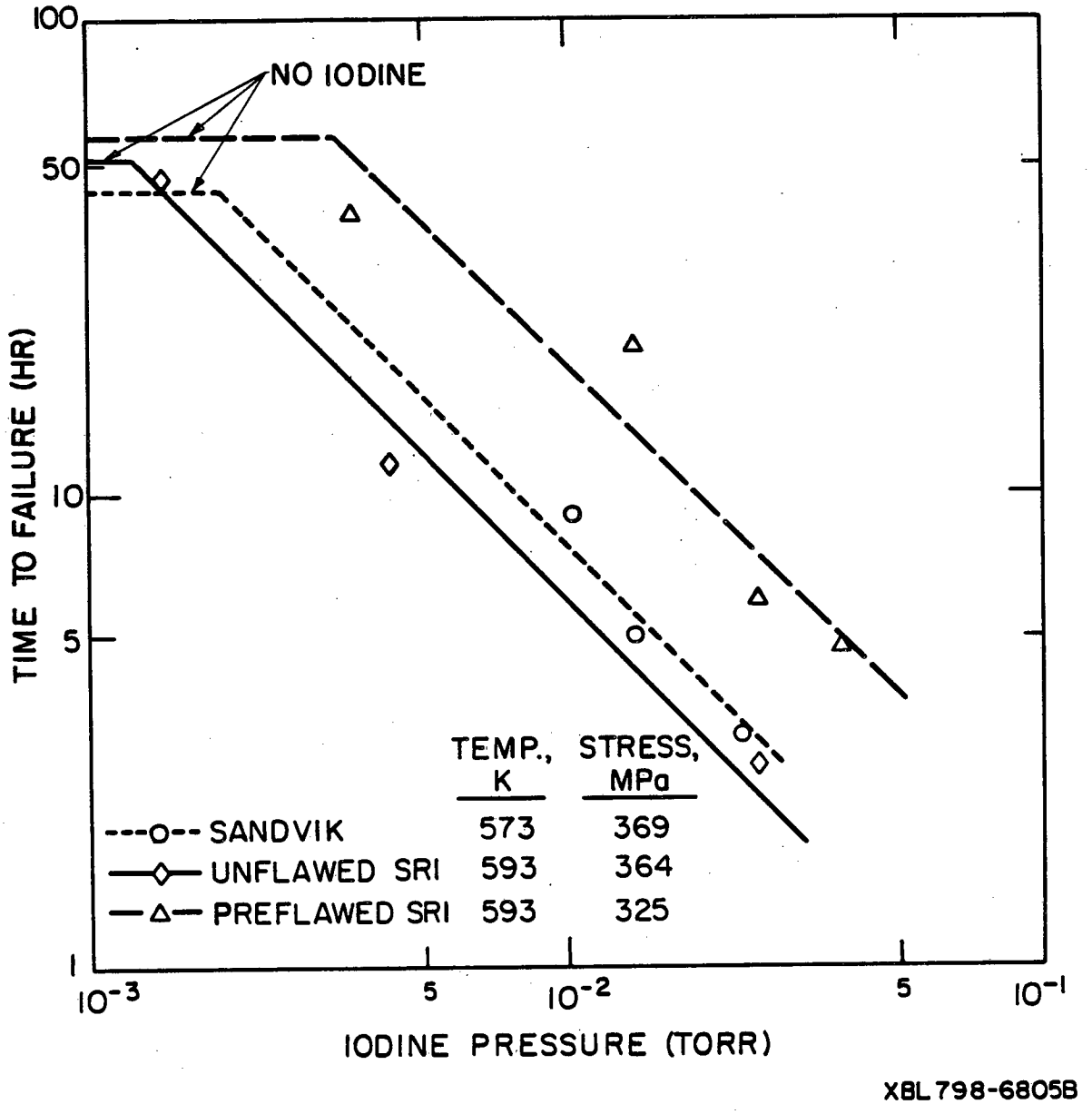
100
50
10
5
1
NO IODINE
TIME TO FAILURE (HR)
TEMP., K
STRESS, MPa
---o-- SANDVIK 573 369
—◇— UNFLAWED SRI 593 364
—△— PREFLAWED SRI 593 325
10-3
5
10-2
5
10-1
IODINE PRESSURE (TORR)
XBL798-6805B

Figure 5

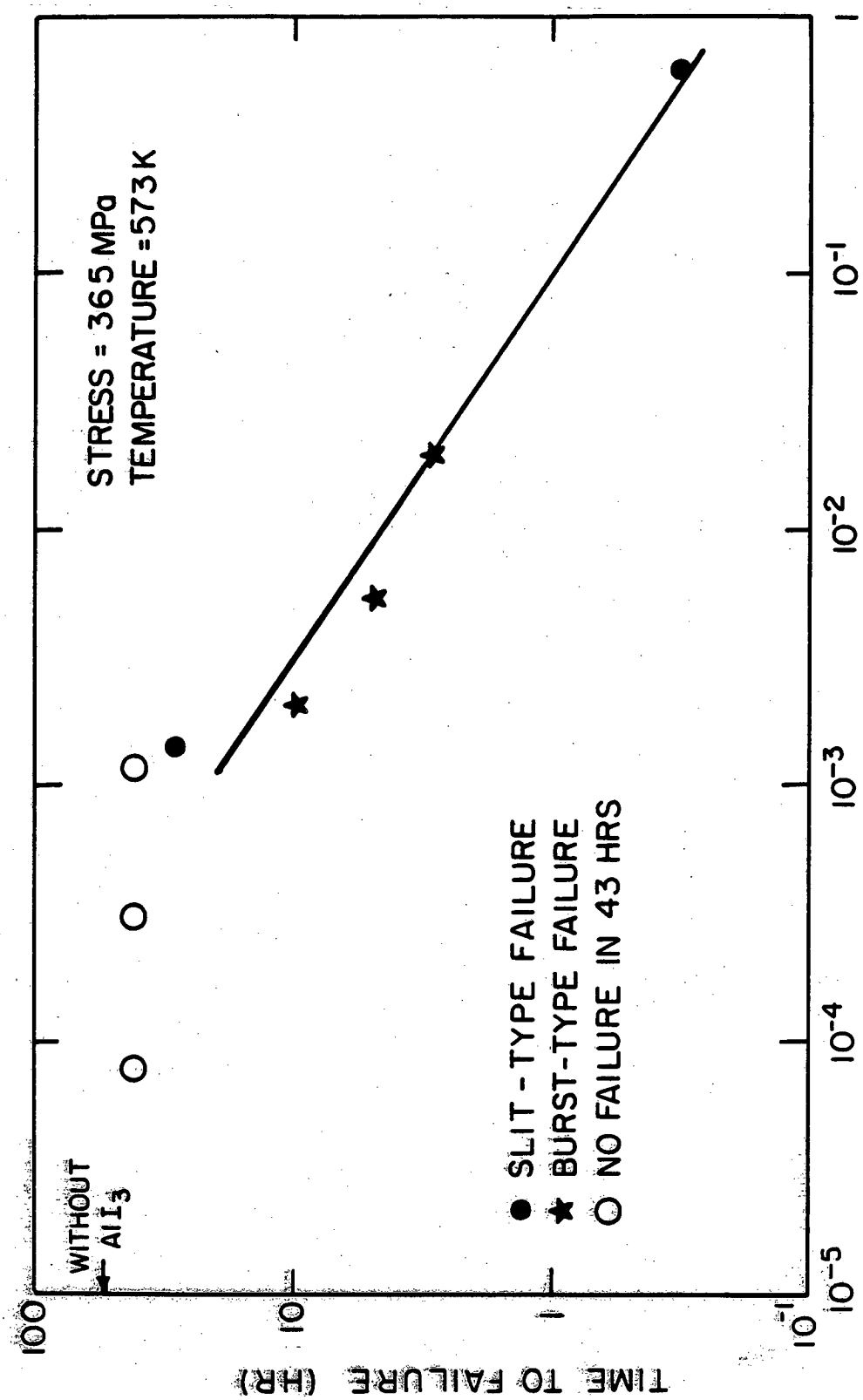

XBL801-4595B

Figure 6

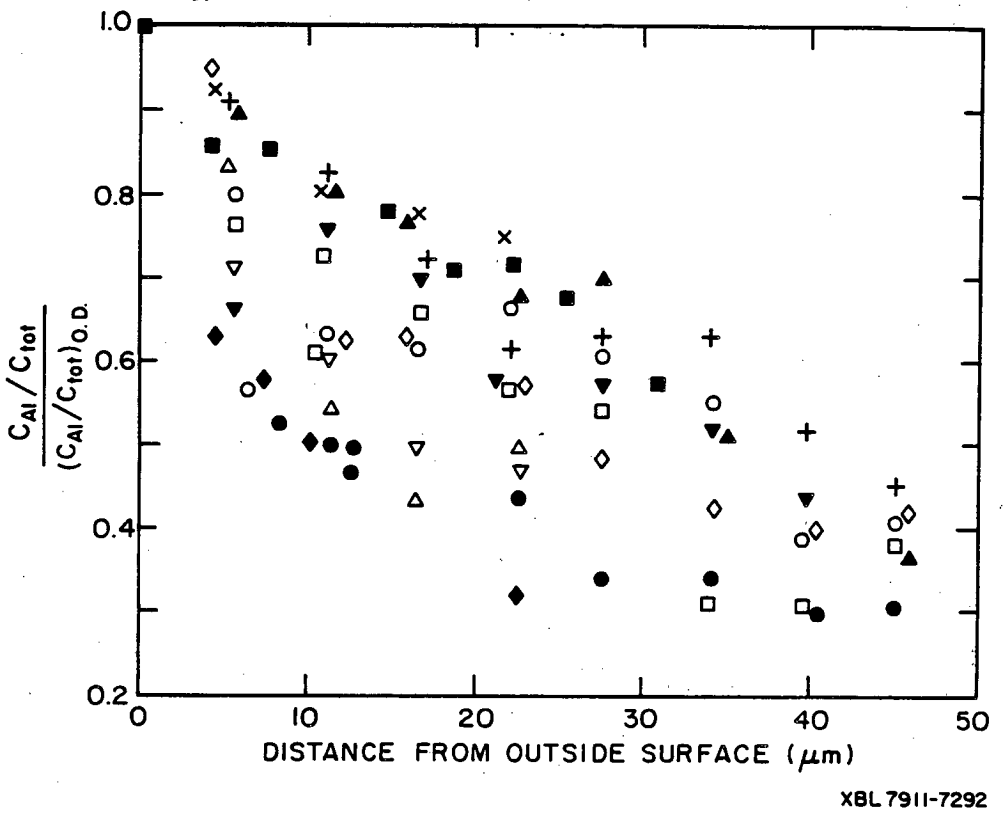

XBL 7911-7292

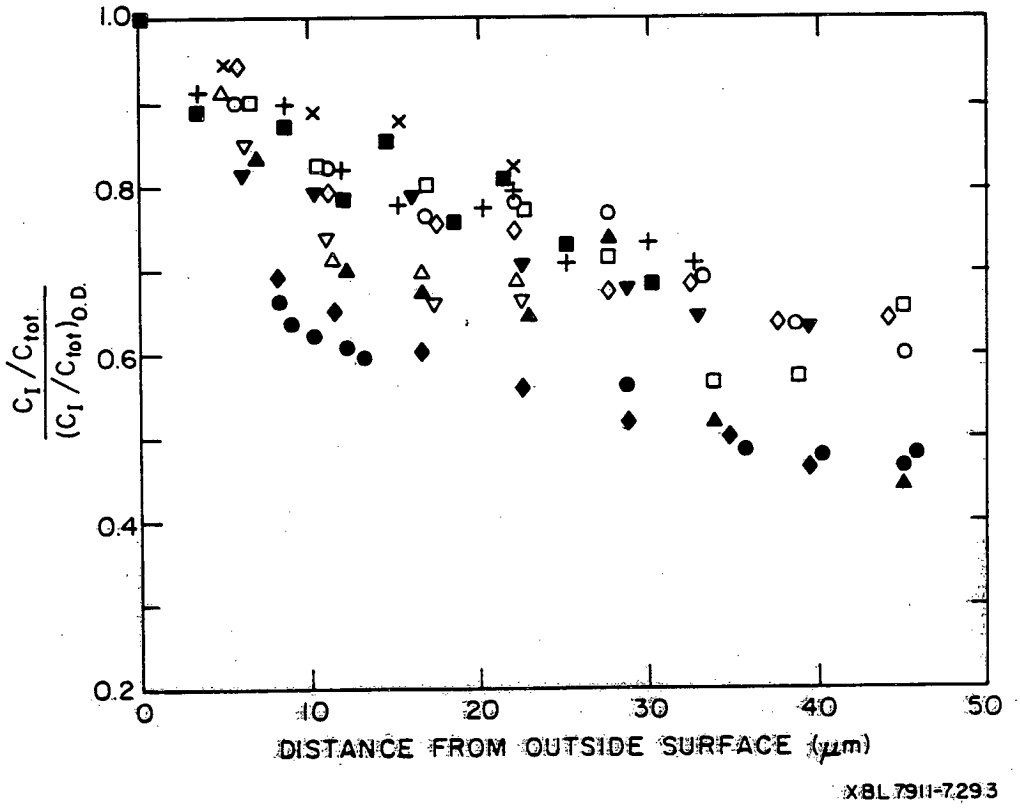

XBL 7911-7293

Figure 7

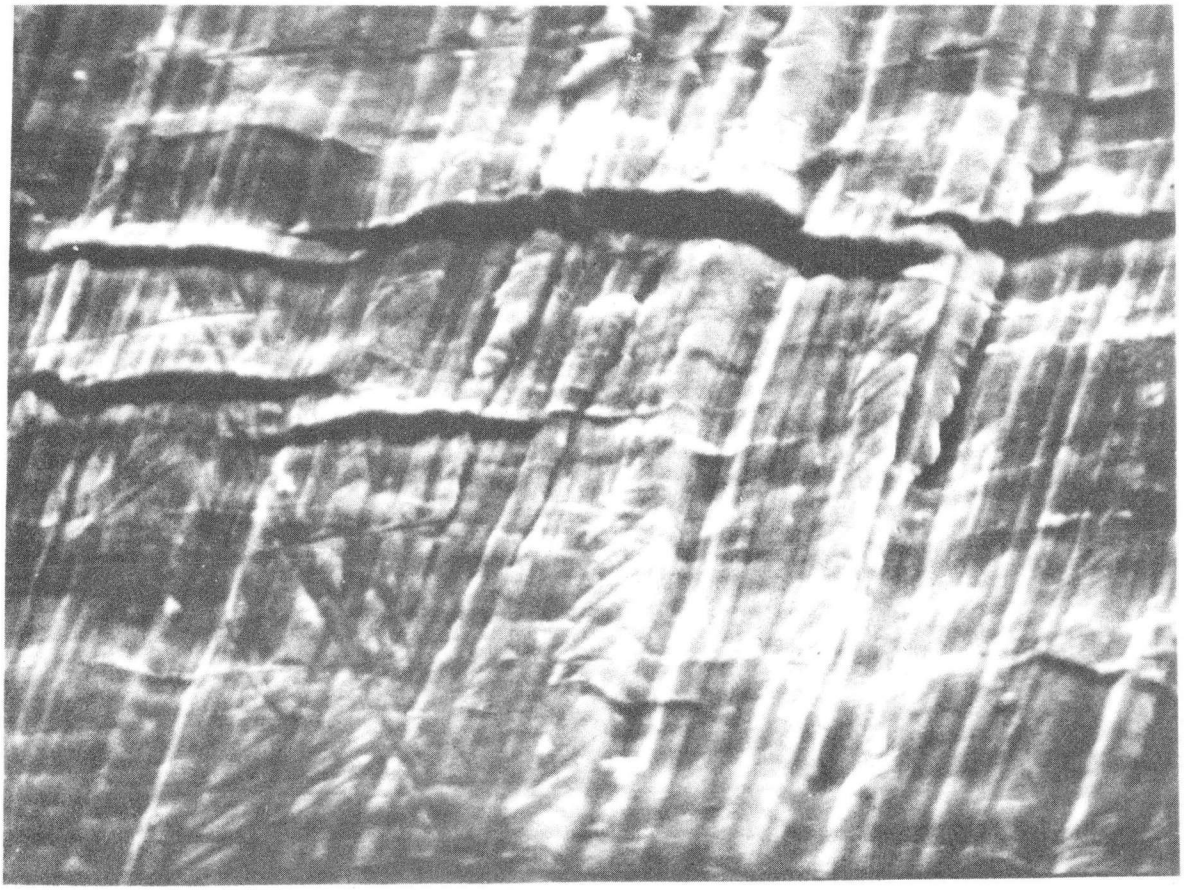

4 μ m

XBB 816-5541

Figure 8 . SEM picture of unfailed specimen under 365 MPa, 300°C, and 3.3×10^{-4} Torr AlI_3 equivalent pressure for 43 hrs.

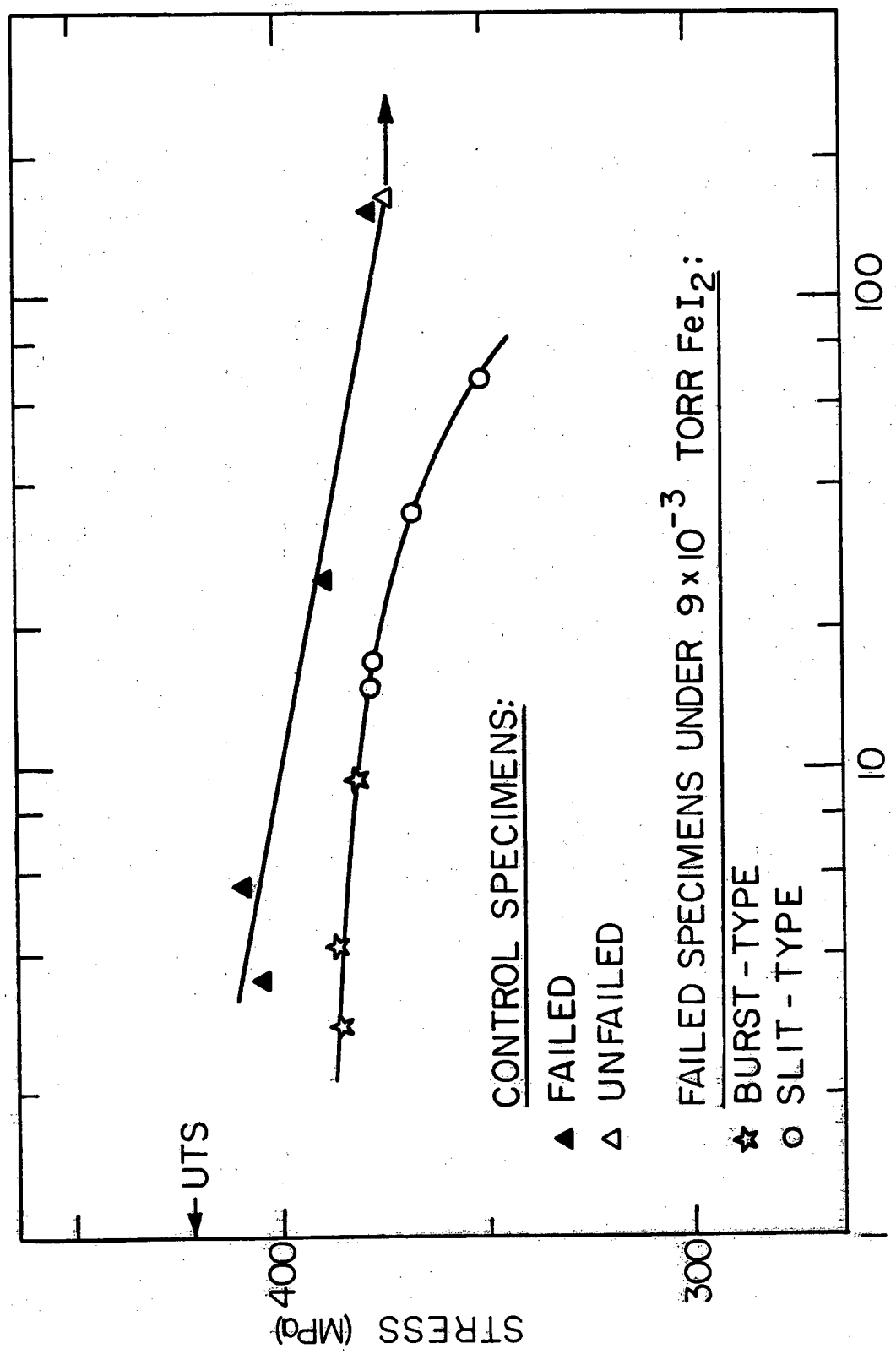

XBL 8012-13431B

Fig. 9

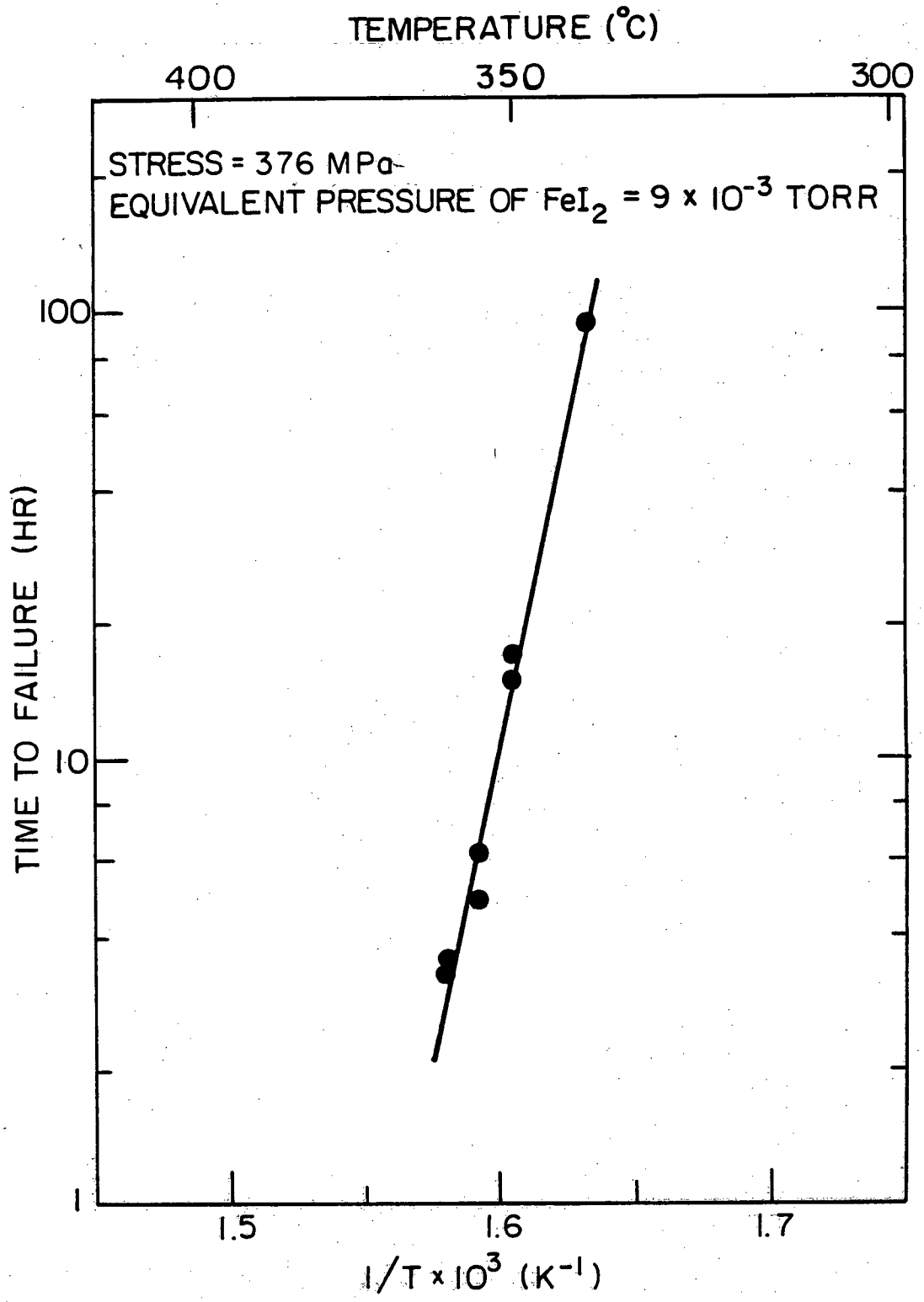
TEMPERATURE (°C)
400
350
300
STRESS = 376 MPa
EQUIVALENT PRESSURE OF FeI_2 = 9 x 10^{-3} TORR
100
10
1
TIME TO FAILURE (HR)
1.5
1.6
1.7
1/T x 10^3 (K^{-1})
XBL 8012-134288

Figure 10

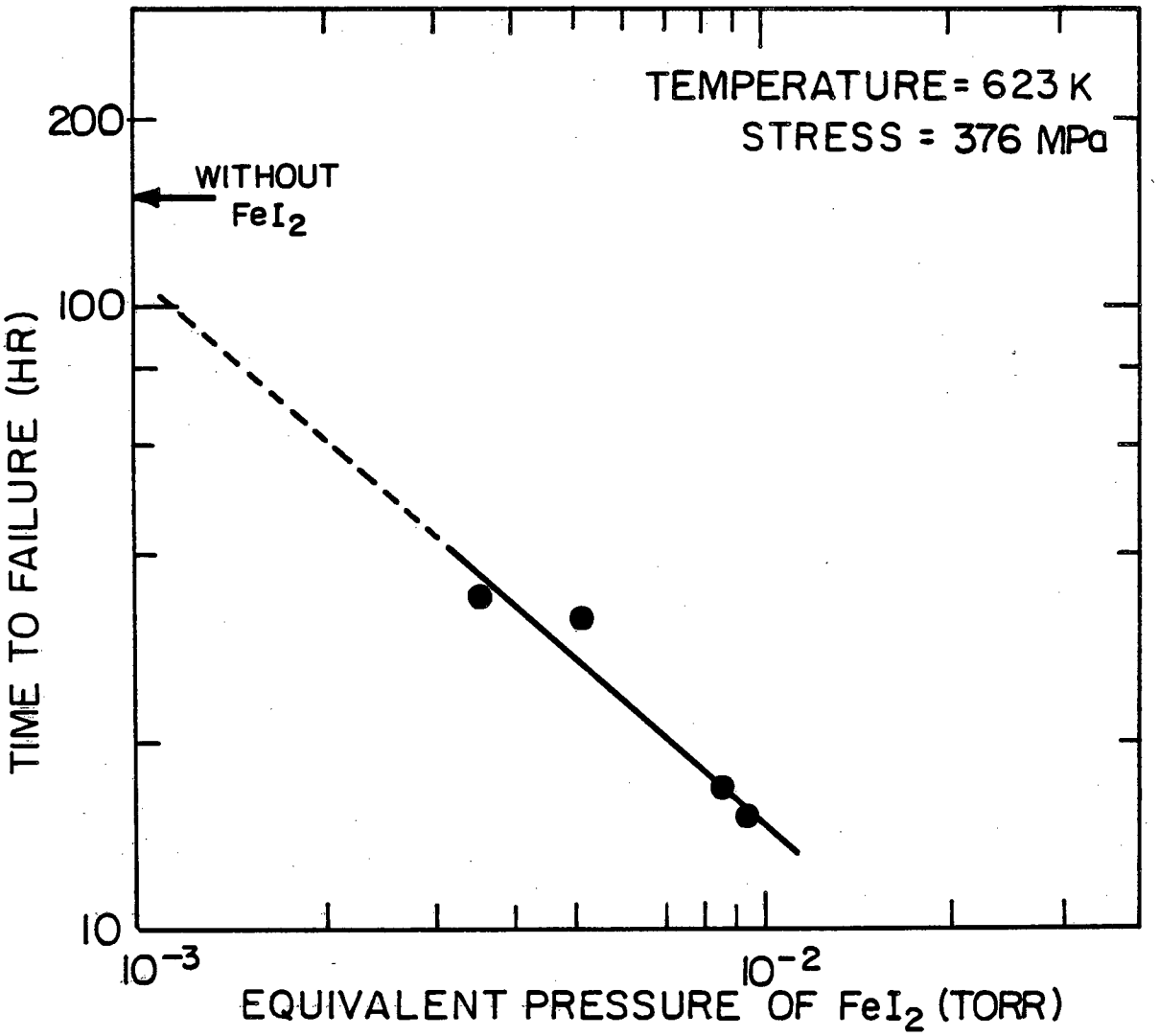
TEMPERATURE = 623 K
STRESS = 376 MPa
WITHOUT
FeI2
200
100
10
TIME TO FAILURE (HR)
10-3
10-2
EQUIVALENT PRESSURE OF FeI2 (TORR)
XBL 8012-134298

Figure 11

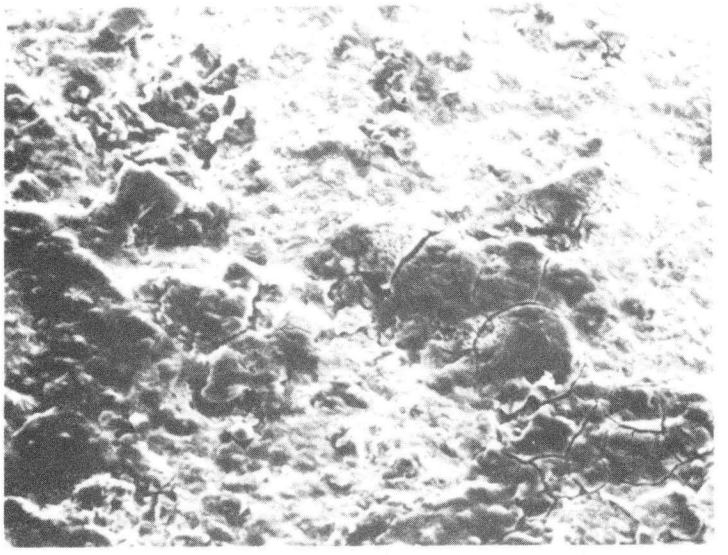

40 μm

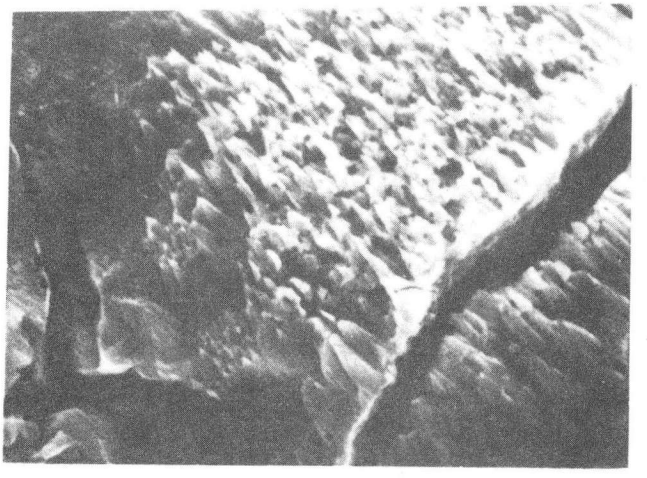

4 μm

XBB 821-253

Figure 12

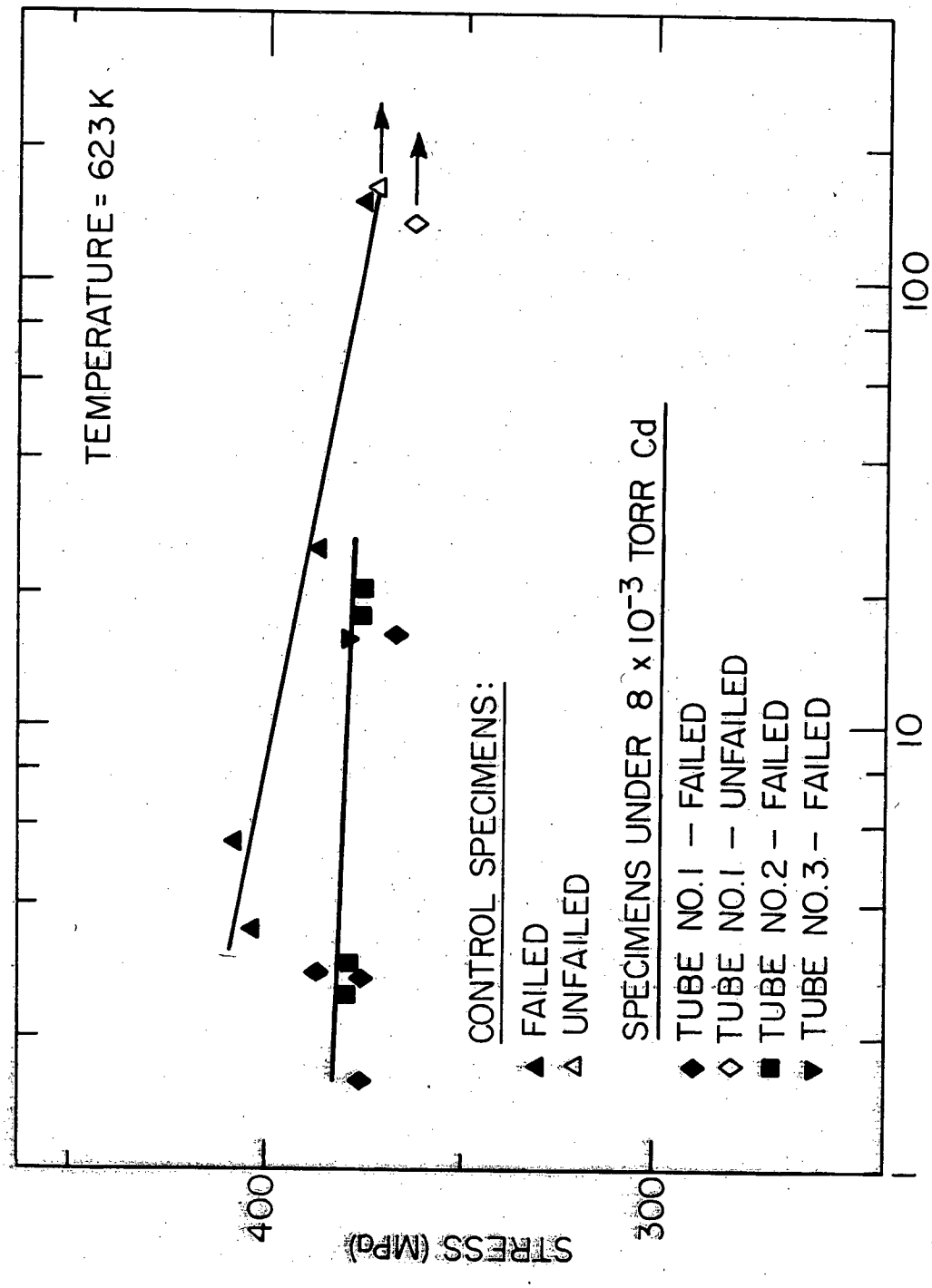

XBL 8012-134308

Fig. 13

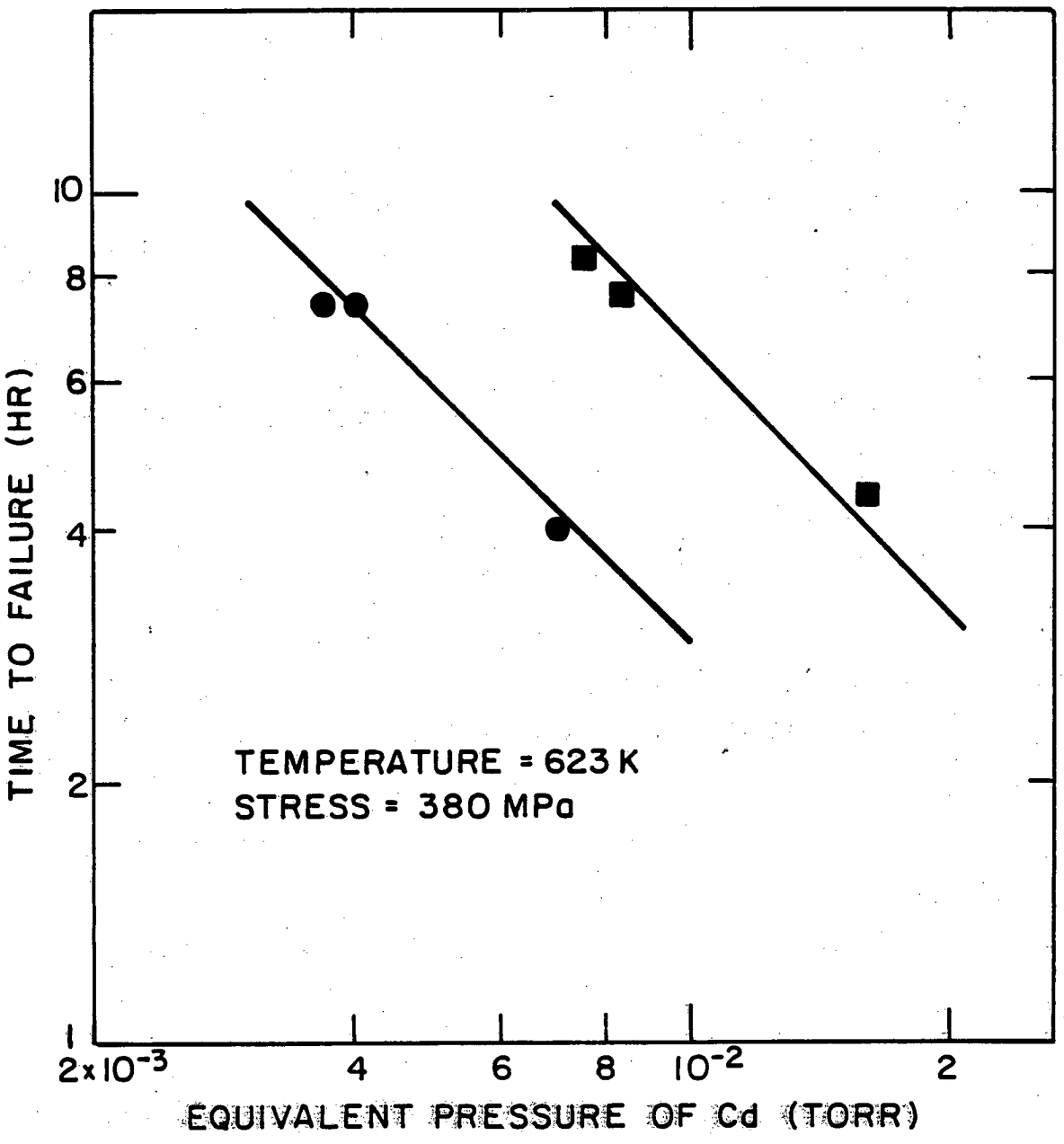

Fig. 14

XBL8112-12890

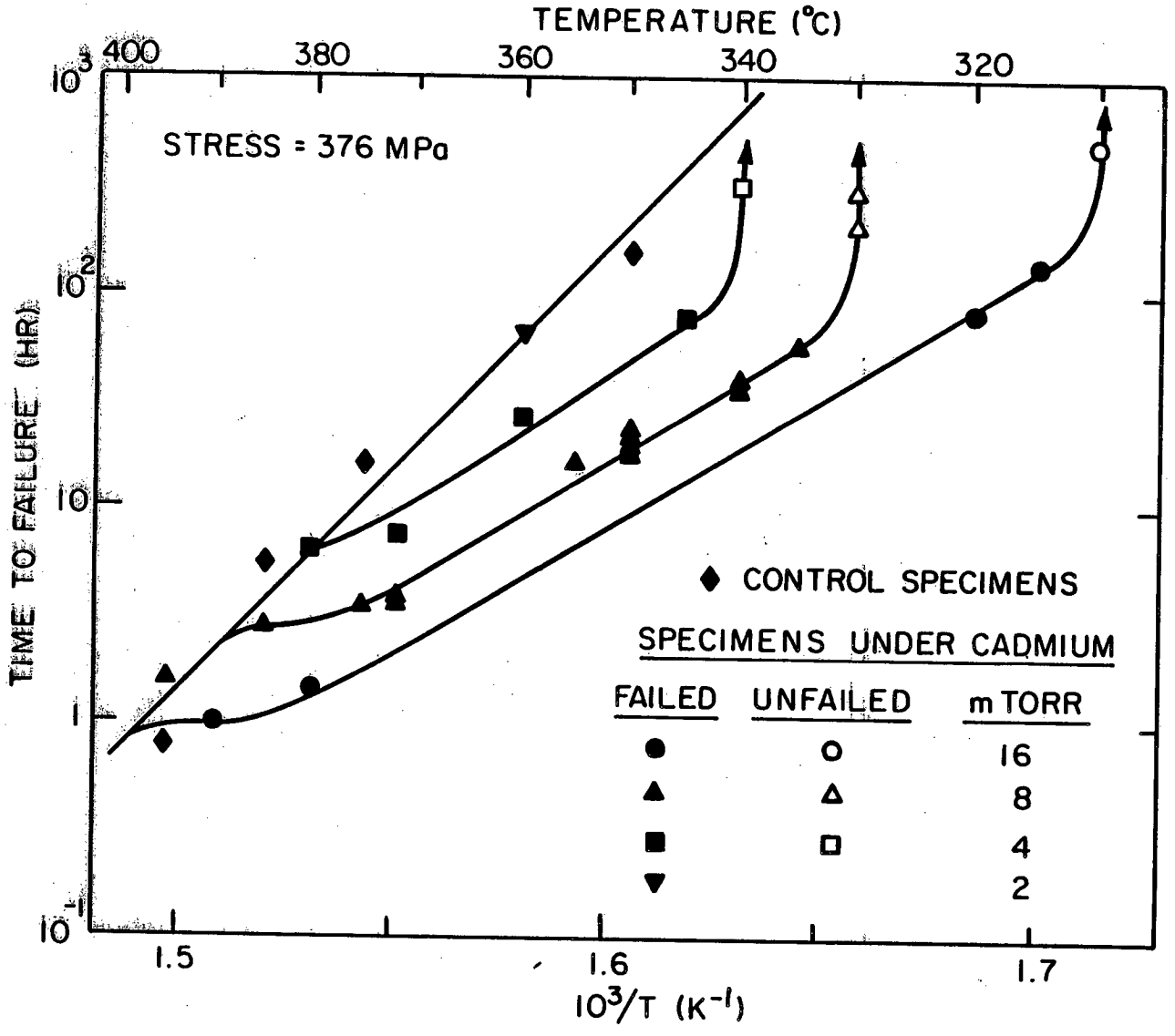

Figure 15 Temperature window study for cadmium vapor embrittlement. XBL 816-6011

TECHNICAL INFORMATION DEPARTMENT
LAWRENCE BERKELEY LABORATORY
UNIVERSITY OF CALIFORNIA
BERKELEY, CALIFORNIA 94720